https://doi.org/10.53656/adpe-2025.13

ROBUST ANALYSIS OF A QUADROCOPTER

Martin Kambushev
Bulgarian Air Force Academy "Georgi Benkovski", Bulgaria
Radoslav Chalakov
National Defence College "Georgi Rakovski", Bulgaria
Desislava Ilieva
Bulgarian Air Force Academy "Georgi Benkovski", Bulgaria

Summary. The report analyzes the singular numbers of a quadcopter. The sensitivity and additional sensitivity in the operating frequency range of the system are studied. The influence of uncertainties of the open and closed system is modeled.
Keywords: singular numbers; sensitivity; additional sensitivity; robust control

1. Introduction

Quadcopters are complex and delicate machines that have entered deeply into modern life. They have found application in almost all spheres of modern life – from photography and videography, industrial inspections, deliveries to agriculture and construction. The war in Ukraine and the conflicts in the Middle East show in practice that unmanned aerial vehicles of any type and size are indispensable on the battlefield (Andonov, 2018; Atanasov, 2024).

As their popularity and complexity grow, so does the need for adequate regulation of their use (Andonov, 2019), and for in-depth analysis of their sustainability and reliability.

Robustness analysis, in the context of quadcopters, is an assessment of their ability to maintain flight stability under conditions of uncertainty and disturbance. These uncertainties can be numerous: variable atmospheric conditions such as wind and turbulence, inaccuracies in sensor data, errors in system modeling, as well as external disturbances such as electromagnetic influences from electronic warfare equipment.

One of the main reasons for the need for robust analysis is to ensure safety. Quadcopters, especially those used in close proximity to people, must be able to be stable and controllable even in the face of unexpected disturbances. Robust analysis helps to identify potential weak points in the system in advance and compensate for them with appropriate algorithms and controllers.

In addition to safety, robust analysis is also essential for improving the accuracy of quadcopters. In many of their applications, such as precision agriculture or

mapping, accurate positioning and stability are required. Robust controllers and control algorithms developed based on robust analysis allow quadcopters to cope with uncertainties and achieve desired results even under variable flight conditions (Madi et al., 2023). Robustness analysis is also important for optimizing the design and development of quadcopters.

By identifying critical parameters and areas of instability, the mechanical structure, sensor system, and control algorithms can be improved to make quadcopters more robust and reliable.

2. Mathematical models of a quadcopter

The created model considers the quadcopter as an absolutely rigid and symmetrical body with 6 degrees of freedom. It consists of 12 nonlinear differential equations that describe the translational motion of the center of mass and the rotation of the body around the center of mass. To describe the translational motion, Euler's differential equations for the change in the amount of motion were used.

$$m\frac{d\vec{V}}{dt} = \sum \vec{F} \tag{1}$$

After equation (1) is developed along the axes of the body-fixed coordinate system, the complete differential equations for the translational motion of the center of mass are obtained:

$$\begin{aligned} \dot{V}_x &= \frac{dV_x}{dt} = \frac{F_x}{m} - \omega_y V_z + \omega_z V_y \\ \dot{V}_y &= \frac{dV_y}{dt} = \frac{F_y}{m} - \omega_z V_x + \omega_x V_z \\ \dot{V}_z &= \frac{dV_z}{dt} = \frac{F_z}{m} - \omega_x V_y + \omega_y V_x \end{aligned} \tag{2}$$

$$\begin{bmatrix} \dot{V}_x \\ \dot{V}_y \\ \dot{V}_z \end{bmatrix} = \frac{1}{m}\begin{bmatrix} -G.sin(\vartheta) \\ f_1 + f_2 + f_3 + f_4 - G.cos(\gamma)cos(\vartheta) \\ G.sin(\gamma)cos(\vartheta) \end{bmatrix} - \begin{bmatrix} 0 & -\omega_z & \omega_y \\ \omega_z & 0 & -\omega_x \\ -\omega_y & \omega_x & 0 \end{bmatrix} \times \begin{bmatrix} V_x \\ V_y \\ V_z \end{bmatrix} \tag{3}$$

where:

G – gravity force directed along the local vertical;

f_1, f_2, f_3, f_4 - forces created by the four engines;

γ, ϑ – roll and pitch angles.

The mutual position between the terrestrial and the body-fixed coordinate systems is determined.

To describe the rotational motion around the axes of the body-fixed coordinate system, the angular momentum change theorem is used.

$$\frac{d\vec{K}}{dt} = \sum \vec{M} \tag{4}$$

To accurately model the motion of aircraft, it is necessary to take into account the dynamics of the change in the lift force and the reactive moment created by each engine. The lift force and the reactive moment are calculated using formula 5. The angular velocity of the rotor *i*, denoted ω_i, creates an axial force f_i. The angular velocity and acceleration of the rotor also create a reactive moment about the rotor axis.

$$\begin{aligned} f_i &= k\omega_i^2, \\ \tau_{M_i} &= b\omega_i^2 + I_M\dot{\omega}_i, \end{aligned} \tag{5}$$

Where:

k is a constant proportional to the thrust. It depends on the geometric characteristics of the propeller;

h is a constant proportional to the reactive torque;

I_M the moment of inertia of the rotor.

The complete equations for rotational motion about the center of mass are:

$$\begin{aligned} \dot{\omega}_x &= \frac{1}{I_x}\left[M_x - (I_z - I_y)\omega_y\omega_z\right]; \\ \dot{\omega}_y &= \frac{1}{I_y}\left[M_y - (I_x - I_z)\omega_z\omega_x\right] \\ \dot{\omega}_z &= \frac{1}{I_z}\left[M_z - (I_y - I_x)\omega_x\omega_y\right] \end{aligned} \tag{6}$$

$$\begin{bmatrix}\dot{\omega}_x \\ \dot{\omega}_y \\ \dot{\omega}_z\end{bmatrix} = \begin{bmatrix}\frac{1}{I_x} & 0 & 0 \\ 0 & \frac{1}{I_y} & 0 \\ 0 & 0 & \frac{1}{I_z}\end{bmatrix}\left[\begin{bmatrix} h(f_4 - f_2) \\ \tau_{M_1} - \tau_{M_2} + \tau_{M_3} - \tau_{M_4} \\ h(f_1 - f_3)\end{bmatrix}\begin{bmatrix}0 & -\omega_z & \omega_y \\ \omega_z & 0 & -\omega_x \\ -\omega_y & \omega_x & 0\end{bmatrix}\begin{bmatrix}I_x & 0 & 0 \\ 0 & I_y & 0 \\ 0 & 0 & I_z\end{bmatrix}\begin{bmatrix}\omega_x \\ \omega_y \\ \omega_z\end{bmatrix}\right] \tag{7}$$

Where:

M_i reactive torque created by the *i* engine;

h – the distance from the center of mass to each of the engines.

The angular position of the quadcopter relative to the ground coordinate system

$M_1X_gY_gZ_g$ is given by three angles: ψ - heading angle, γ - roll angle, ϑ - pitch angle. The relationship between these angles and the angular velocities around the axes of the coordinate system associated with the aircraft is given by the following differential equations:

$$\begin{bmatrix}\dot{\psi}\\ \dot{\gamma}\\ \dot{\vartheta}\end{bmatrix} = \begin{bmatrix}\frac{\omega_y \cos\gamma + \omega_z \sin\gamma}{\cos\vartheta}\\ \omega_x + \tan\vartheta\left(\omega_y \cos\gamma + \omega_z \sin\gamma\right)\\ \omega_y \sin\gamma + \omega_z \cos\gamma\end{bmatrix} \tag{8}$$

The spatial displacement of the aircraft is described by a standard matrix of steering cosines and linear velocities in the body-fixed coordinate systems.

$$\begin{bmatrix}\dot{X}\\ \dot{Y}\\ \dot{Z}\end{bmatrix} = C_{(\psi,\gamma,\vartheta)}\begin{bmatrix}V_x\\ V_y\\ V_z\end{bmatrix}. \tag{9}$$

The system of differential equations describing the motion of the quadcopter consists of the expressions (3, 7, 8, 9). The state vector contains the following variables $\left(V_x V_y V_z \omega_x \omega_y \omega_z \psi\gamma\vartheta XYZ\right)$.

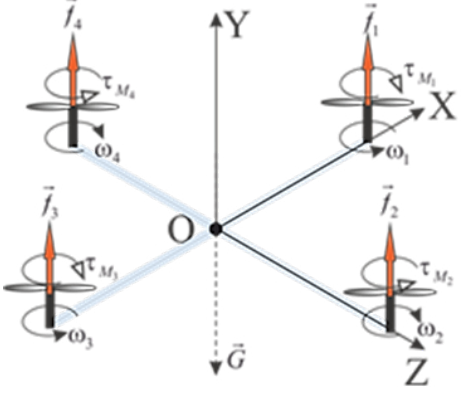

Figure 1. The distribution of external forces and moments acting on a quadcopter

Based on the systems of equations (3, 7, 8, 9), a nonlinear model of a quadcopter was created in SIMULINK, shown in Figure 2.

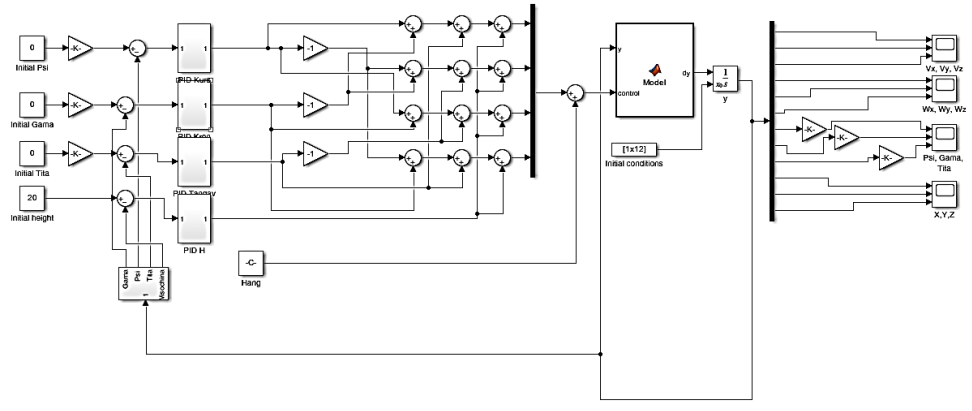

Figure 2. Model of a quadcopter

For the purposes of robust analysis, linearization was performed using the partial derivative method of the nonlinear model and a description of the quadcopter in state space was obtained – formulas 10 and 11.

$$A = \begin{bmatrix} 0 & a_{12} & a_{13} & 0 & a_{15} & a_{16} & 0 & 0 & a_{19} \\ a_{21} & 0 & a_{23} & a_{24} & 0 & a_{26} & 0 & a_{28} & a_{29} \\ a_{31} & a_{32} & 0 & a_{34} & a_{35} & 0 & 0 & a_{38} & a_{39} \\ 0 & 0 & 0 & 0 & a_{45} & a_{46} & 0 & 0 & 0 \\ 0 & 0 & 0 & a_{54} & 0 & a_{56} & 0 & 0 & 0 \\ 0 & 0 & 0 & a_{64} & a_{65} & 0 & 0 & 0 & 0 \\ 0 & 0 & 0 & 0 & a_{75} & a_{76} & 0 & a_{78} & a_{79} \\ 0 & 0 & 0 & a_{84} & a_{85} & a_{86} & 0 & a_{88} & a_{89} \\ 0 & 0 & 0 & 0 & a_{95} & a_{96} & 0 & a_{98} & 0 \end{bmatrix} \quad (10)$$

$$B = \begin{bmatrix} 0 & 0 & 0 & 0 \\ b_{21} & b_{22} & b_{23} & b_{24} \\ 0 & 0 & 0 & 0 \\ 0 & b_{42} & 0 & b_{44} \\ b_{51} & b_{52} & b_{53} & b_{54} \\ b_{61} & 0 & b_{63} & 0 \\ 0 & 0 & 0 & 0 \\ 0 & 0 & 0 & 0 \\ 0 & 0 & 0 & 0 \end{bmatrix} \quad (11)$$

For the chosen state vector including $(V_x V_y V_z \omega_x \omega_y \omega_z \psi \gamma \vartheta XYZ)$, the system is completely observable because all its components are measured in flight. Therefore, the matrix C is a unit matrix of dimension (9x9): C=E. The matrix D is zero because there is no direct connection between the input and the output.

3. Singular analysis

Using the resulting linear model described in state space, an analysis of the singular numbers of the quadcopter was performed in the frequency range $[10^{-2} \div 10^{2}] rad/s$, which represents the operating frequency range of the quadcopter.

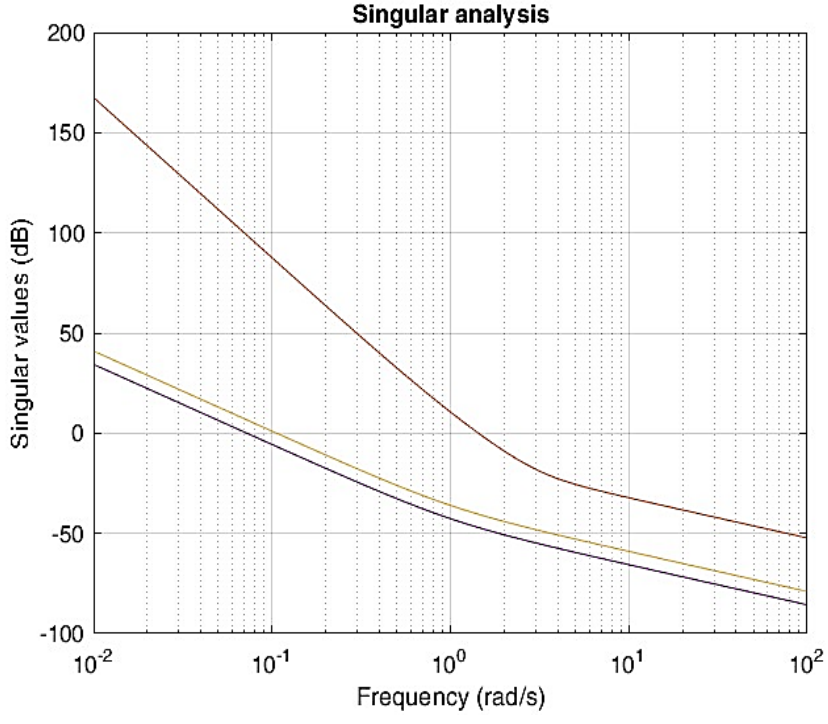

Figure 3. Singular analysis

Analysis of different frequency ranges:

● Low frequencies $[10^{-2} \div 10^{-1}]rad/s$:

In this area, the singular values are highest. This indicates that the system is most sensitive to low-frequency input signals, which can be interpreted as the system's response to very slow changes in the input signals

● Mid-range frequencies$[10^{-1} \div 10^{1}]rad/s$:

In this area, the singular values decrease rapidly. This indicates that the gain of the system decreases with increasing frequency. In this region, the system changes its behavior abruptly.

● High frequencies$[10^{1} \div 10^{2}]rad/s$:

In this area, the singular values continue to decrease and stabilize. In this region, the system is the least sensitive. This indicates that the system is less sensitive to high frequency input signals.

Figure 3 shows three graphs, but in reality there are four. These are the heading, roll, pitch, and altitude control channels.

The red curve, which has the highest gain, represents the roll and pitch channel. The coincidence of the two curves is due to the complete coincidence and symmetry of the quadcopter with respect to roll and pitch.

4. Analysis of the sensitivity S and the additional sensitivity T of the quadcopter

4.1. Sensitivity (S):

Stability:

The sensitivity S (Skogestad & Postlethwaite, 2005) indicates how disturbances are transmitted through the system.

High values of S in a particular frequency range indicate that the system is sensitive to disturbances in that range.

Peaks in S may indicate resonant frequencies that can lead to a decrease in the stability of the quadcopter.

Controllability:

S also affects the ability of the quadcopter to suppress disturbances that can interfere with precise control.

High values of S may result in unwanted movements or vibrations that make control difficult.

4.2. The additional sensitivity (T):

Stability:

T indicates how the reference signal is transmitted through the system.

High values of T in the high frequency range can lead to noise amplification, which can reduce stability.

Peaks in T can also indicate resonant frequencies, which can lead to instability.

Controllability:

T affects the ability of the quadcopter to track the reference signal.

High values of T in the low frequency range are desirable for good tracking of the reference signal.

Low values of T in the high frequency range are desirable to reduce noise amplification.

4.3. Interaction between S and T:

S and T are related by the equation $S + T = I$, where I is a unit matrix.

This means that the controller of any real system, in this case a quadcopter, must balance between suppressing interference and tracking the reference signal.

The design of a quadcopter controller requires a careful balance between S and T to ensure both stability and controllability.

The created linear model allows for the study of the sensitivity S and the additional sensitivity T. As a result of the study, a matrix of size [12X12] containing Bode plots of S and T was obtained.

Figures 4, 5 and 6 show part of the obtained Bode characteristics of S and T.

The graphs shown, in which high values of S are observed in the low-frequency range, mean that the drone is susceptible to interference and is not very stable, which leads to difficulty in its control.

From the graphs, where high T values are observed in the low-frequency range, it means that the drone has good tracking of the reference signal, which is good for its controllability.

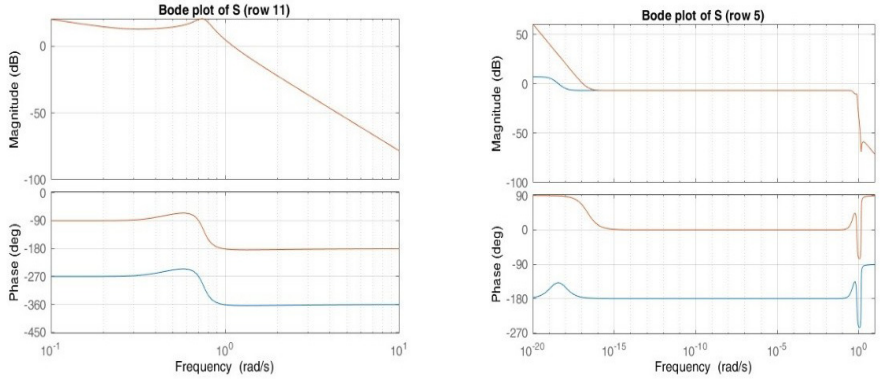

Figure 4. Bode diagrams of sensitivity S(blue) and additional sensitivity T(red)

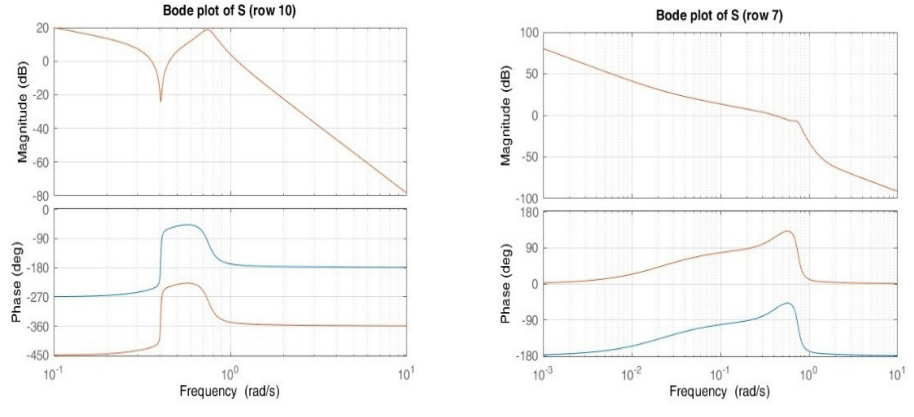

Figure 5. Bode diagrams of sensitivity S(blue) and additional sensitivity T(red)

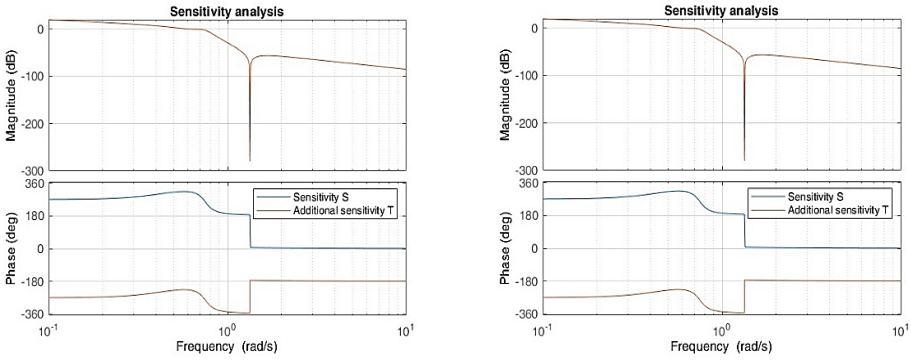

Figure 6. Bode diagrams of sensitivity S(blue) and additional sensitivity T(red)

5. Studying the influence of uncertainties on the behavior of the quadcopter

The created model, shown in Figure 2, is a closed system with PID controllers. Studies have been made of the open and closed system with PID controllers.

The behavior of both systems was studied under changes in mass, moments of inertia, the coefficient k – through which the thrust of the individual engines is modeled (shown in formula 5) and the influence of atmospheric disturbances – for this purpose the Dryden Wind Turbulence Mode from Simulink was used.

The initial conditions of the simulation are:

$$V_x = 0; V_y = 0; V_z = 0; \omega_x = 0; \omega_y = 0; \omega_z = 0; \psi = 0; \gamma = 0; \vartheta = 0; X = 0; Y = 0; Z = 20;$$

The simulation results show that changes in mass in the open system lead to a smooth decrease or increase in flight altitude. In the closed system, changes in mass are compensated by the PID controllers until the maximum thrust of the engines is reached. Changes in the moments of inertia have no effect in both models. Changes in the coefficient k by 5% of one of the engines lead to the following changes:

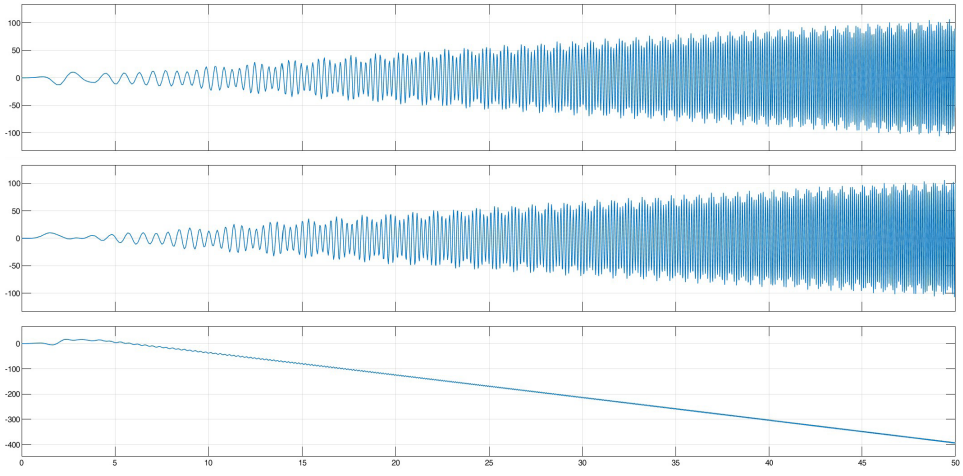

Figure 7. Influence of the coefficient k on V_x, V_y, V_z of the open system

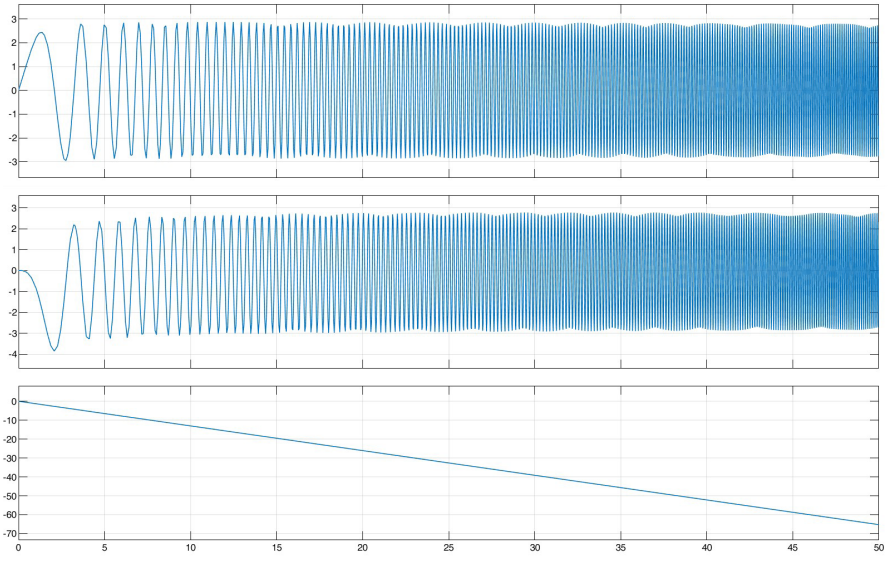

Figure 8. Influence of the coefficient k on $\omega_x, \omega_y, \omega_z$ *of the open system*

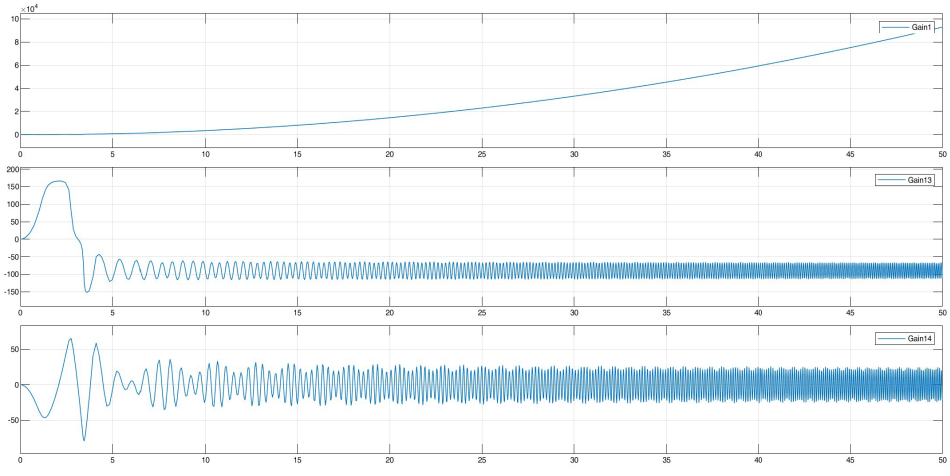

Figure 9. Influence of the coefficient k on ψ, γ, ϑ of the open system

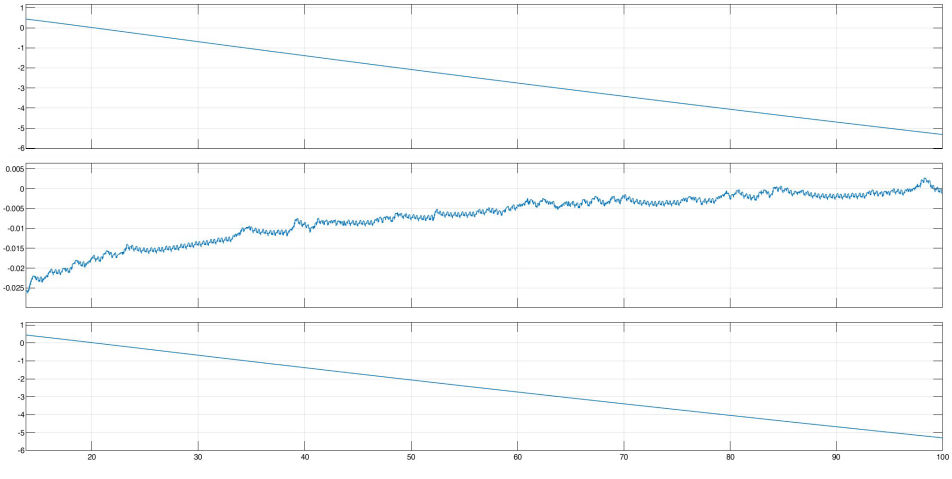

Figure 10. Influence of the coefficient k on V_x, V_y, V_z of the closed system

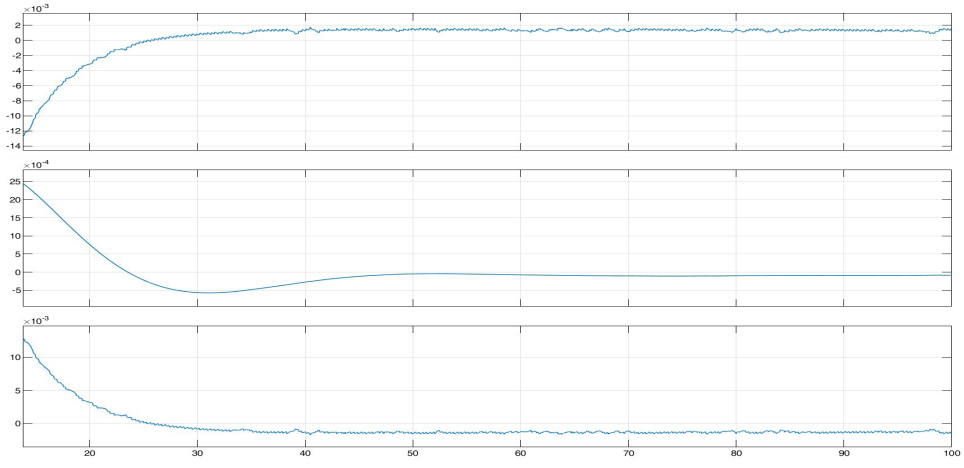

Figure 11. Influence of the coefficient k on $\omega_x, \omega_y, \omega_z$ of the closed system

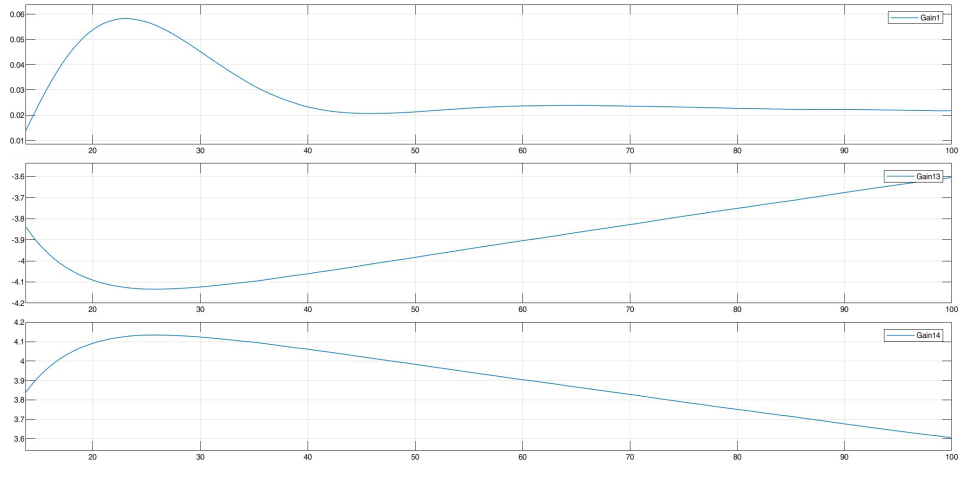

Figure 12. Influence of the coefficient k on ψ, γ, ϑ of the closed system

Figures 7÷12 show the effect of a 5% reduction in the thrust coefficient of one of the engines on elements of the state vector. Figures 7÷9 sequentially show the changes in $V_x, V_y, V_z, \omega_x, \omega_y, \omega_z, \psi, \gamma, \vartheta$ of the open system, and figures 10÷12 of the closed system.

The influence of turbulence is shown in Figure 13.

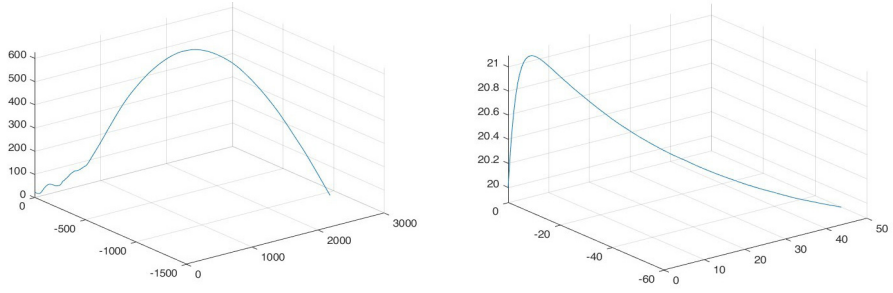

a) **b)**

Figure 13. Influence of turbulence a) open system, b) closed system

Conclusions

● In the low frequency region, we have high values of S and T. This indicates that the system is sensitive to both disturbances and reference signals in this area.

● In the high frequency range, the gain of S and T is also low. This indicates that the system is less sensitive to both disturbances and reference signals in this area.

● The peaks in S and T values appear in the same frequency regions, indicating that the resonant frequencies affect both the interference and reference signals.

● Analysis of Bode plots allows to identify frequency ranges in which the system is sensitive to disturbances or has problems tracking the reference signal.

Figures 7 ÷ 12 show the sensitivity of the system to uncertainties. Their analysis leads to the following conclusions:

● The quadcopter, as an open system, is unstable and does not possess robust stability.

● The closed system is stable and has a certain robustness with respect to uncertainties and external disturbances.

For the safe use of quadcopters in urban areas, it is necessary to use combined controllers with a robust (Zhou et al., 1996) and an adaptive component in their control. The combined robust-adaptive controller offers a solution that guarantees stability and adaptability to unpredictable disturbances and changing conditions.

Acknowledgements

The research in this article was carried out in fulfillment of Task 3.1.9. "Construction of a network of autonomous low-powered aerial devices (quadracopters) for control of an urbanized area" by the National Scientific Program "Security and Defense", adopted by RMS No. 731 of 21.10.2021. and according to Agreement No. D01-74/19.05.2022."

REFERENCES

Andonov, A. (2019). "Open" Category Unmanned Aerial Systems Harmonized Standards and Requirements Complex. *Proceedings of the International Scientific Conference*, *25*(3), 74 – 80. https://doi.org/10.2478/kbo-2019-0121.

Andonov, A. (2018). A model for determining the optimal quantity of ImBLA when overcoming an enemy air defense system. *Modern aspects of security - challenges, approaches, solutions, Collection of reports from the annual VNK with international participation of the Faculty of Command and Staff, 20 – 21.06.2018, Military Academy "Georgi S. Rakovski"*, 198 – 206.

Atanasov, M. (2024). Possibilities for Improving Algorithms for Combat Use of Aircraft Using Unguided Weapons. *The Eurasia Proceedings of Science Technology Engineering and Mathematics*, *28*, 428 – 437. https://doi.org/10.55549/epstem.1523628.

Skogestad, S., Postlethwaite, I. (2005). *Multivariable feedback control: analysis and design*. John Wiley & Sons.

Madi, S., Larabi, M., Kherief, N. (2023). Robust control of a quadcopter using PID and H controller. *Turkish Journal of Electromechanics & Energy*, *8*(1), 3 – 11.

Zhou, K., Doyle, J. C., Glover, K. (1996). *Robust and optimal control*. Prentice Hall.

✉ **Ch. Assist. Prof. Martin Kambushev, PhD**
ORCID iD 0000-0002-7681-4524
Bulgarian Air Force Academy "Georgi Benkovski"
Dolna Mitropolia, Bulgaria
E-mail: mkambushev@af-acad.bg

✉ **Ch. Assist. Prof. Radoslav Chalakov, PhD**
ORCID iD: 0000-0001-6780-9136
National Defence College "Georgi Rakovski"
Command and Staff Faculty
Sofia, Bulgaria
E-mail: r.chalakov@rndc.bg

✉ **Assist. Desislava Ilieva**
Bulgarian Air Force Academy "Georgi Benkovski"
Dolna Mitropolia, Bulgaria
E-mail: dilieava@af-acad.bg